Determination of Vibration Characteristics of Hypo & Hyper Eutectic "Al-Si" Alloys

Somashekar V[1]

[1]*Asst. Professor, Department of Aeronautical Engineering, ACSCE, Bangalore-560074, India*

ABSTRACT

Vibration is an effective tool in detecting and diagnosing some of the incipient failures of machine and equipment. Vibration signature measured on the external surface of the machine or a structure contains a good amount of information, which if properly interpreted, can reveal the running condition of the machine. It may be regarded as the one of the languages through which the machine tells its ailments. Each unit of mechanical equipment has a different signature in the frequency spectrum. The vibration spectrum shows the areas of stress and undue energy. Vibration measurements trend changes at different locations along the units to predict problems. Vibration analysis can determine misalignment, unbalance, mechanical looseness, eccentric shafts, gear wear, broken teeth, bearing wear etc. Using appropriate accelerometer it is possible to get the data which is processed using different methods like FFT, spectrogram, cestrum, and wavelet transform and cyclostationary analysis.

In this work both analytical and experimental approach to the modal analysis provides sufficient information about the modal behaviour. Rigorous work involved in modelling and analysis has been done using ANSYS workbench. The analysis aims at predicting modal behaviour.

Key words: Fast Fourier Transformation (FFT), Ansys workbench, Monitoring Equipment Uptime, Damping frequency, Vibration Characteristics.

1. Introduction

Engineering systems possessing mass and elasticity are capable of relative motion. If motion of such systems repeats itself after a given interval of time, the motion is known as vibration.

In the simplest form vibration can be considered to be oscillation or repetitive motion of an object around an equilibrium position. The equilibrium position is the position the object will attain when the force acting on it is zero. When elastic bodies such as spring, a beam and a shaft are displaced from the equilibrium position by the application of forces, and then released, they execute a vibratory motion. This is due to the reason that, when a body is displaced, the internal forces in the form of elastic or strain energy are present in the body. At release, these forces bring the body to its original position. When the body reaches the equilibrium position, the whole of the elastic or strain energy is converted into kinetic energy due to which the body continues to move in the opposite direction. The whole of the kinetic energy is again converted into strain energy due to which the body again returns to the equilibrium position. In this way, vibratory motion is repeated indefinitely in the absence of damping.

1.1 Methods of vibration control

The various methods of vibration control aim at modifying the source or the system or the transmission path from the source to the system are explain in the below Fig 1.1. This vibration control method sometimes uses an active control circuit.

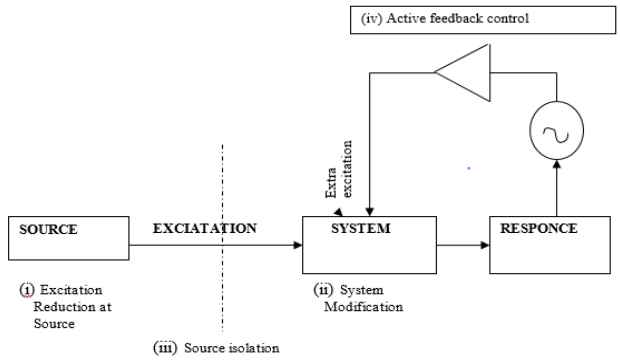

Figure 1.1: Methods of vibration control

The first group of method attempts to reduce the excitation level at the source. This method is very effective and should be applied in the case of balancing of inertia forces, smoothening of fluid flow (when the vibration is flow-induced), proper lubrication at joints, etc. For a self-excited system, a suitable modification of the system parameters may also reduce the excitation level.

A large number of method exist in the second group i.e., system modification. In this method, the system parameters like inertia, stiffness, and damping are suitably chosen and modified to reduce the response to a given excitation. The system parameters are effectively controlled by both the geometry and material of the vibrating member, i.e., by structure design and redesign. A very useful remedial method in this group requires the application of the dynamic vibration absorber.

The third group of methods, modified the transmission path of vibration and properly known as isolation. For the isolation purpose an appropriate suspension system or anti vibration mount (in the form of a resilient element) is inserted in the path of vibration transmission from the source of the system.

1.2 Basic Principle Involved

i. Any malfunctioning or deterioration in the operation of machine component gives rise to increase in vibration level.
ii. Vibration emanating from the component consists of certain frequencies depending upon the nature of the operation. This frequency does not get changed or lost during the transmission of vibration. However there vibration level may be attenuated.
iii. Mixing of different vibration (frequencies) does not cause any loss of individual frequency information.
iv. Every individual component or a system has its own frequency called natural frequency, which changes only when system parameter affected.

1.3 Vibration Analysis Process

A vibratory system is a dynamic system for which the variable such as excitations (inputs) & responses (outputs) are time dependent. The response of a vibrating system generally depends on the initial conditions as well as external excitations. Thus the analysis of a vibrating system usually involves mathematical modelling, derivation of the governing equations, solution of the equations, and interpretation of the results.

Step 1: Mathematical modelling

The purpose of the mathematical modelling is to represent all the important features of the system for the purpose deriving the mathematical or analytical equations governing the behaviour of the system. The mathematical model should include enough details to describe the system in terms of equations without making it too complex.

Step 2: Derivation of governing equation

Once the mathematical model is available, we use the principle of dynamics and derive the equations that describe the vibration of the system. The equation of motion can be derived conveniently by drawing the free-body diagram of all the mass involved. The free-body diagram of a mass can be obtained by isolating the mass and indicating all externally applied forces, the reactive forces, and the inertia forces.

Step 3: Solution of the governing equation

The equation of the motion must be solved to find the response of vibrating system. Depending on the nature problem, we can use any one of the following techniques for finding the solution: standard methods of solving differential equations, Laplace transformation methods, matrix methods, and numerical methods.

Step 4: Interpretation of the results

The solution of the governing equation gives the displacements, velocities and accelerations of the various masses of the system. These results must be interpreted with a clear view for the purpose of the analysis and the possible design implications of the results.

2. Methodology

In this work both analytical and experimental approach to the modal analysis provides sufficient information about the modal behaviour.

One approach is the analytical method starting from the structural geometry, the boundary conditions and material characteristics i.e. mass, stiffness and damping distribution of the structure is expressed in terms of respective matrices. These contain sufficient information to determine the system modal parameters. In this work used ANSYS workbench.

The experimental approach starts from the measurement of dynamic input forces and output response of the structure of interest. These

measurements are often transformed into frequency response functions. They can be expressed in terms of modal parameters.

An experimental modal analysis consists of five phases such as.

i. **Building the test set up:** Suspending test object, attaching transducers, connecting the data acquisition system, calibration.
ii. **Acquisition of the data:** Most often, the estimation of frequency response functions.
iii. **System identification phase:** The determination of vibration characteristics of the system from the measured input–output data.
iv. **Validation of the obtained results**
v. **Improving vibration characteristics test model:** All the above phases are necessary to reach the fifth phase. Using the obtained information we can improve the system in a systematic way.

3. Experimental Setup

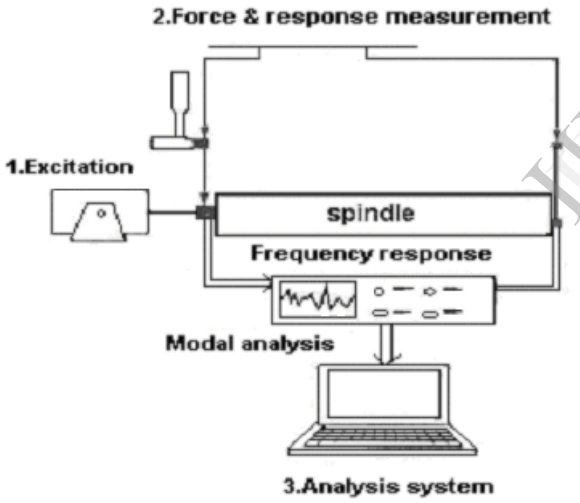

Figure 3.1: Experimental setup

The different aspects of classical experimental modal analysis each depending specific tools as shown in the Fig 3.1. In a modal analysis test a vibration force has to be applied to the structure. An exciter system or a hammer impact serves this purpose. Force transducer will measure the (input) force. Motion transducer measures the (output) vibration motion. These signals are processed by an analysis system that will digitize them and use them for estimation on the frequency response function. This procedure is repeated for several excitation and response combinations. All frequency response functions are stored on a disc memory of the analysis system. During the next phase, the analysis system will determine the modal characteristics (system poles, mode shape vectors, participation function) of the structure under investigation, based upon the measured frequency response function. Animation graphical tool will simulate on the screen the modal deformations based upon a wire frame model.

3.1 Instrumentations

Exciter systems: In this work Model 086C40 (IMI Sensors) impact hammer has been used. The hammer has the following specifications:

- 8000 Hz frequency range 2200N amplitude range
- *2.3 mV/N sensitivity*
- *0.14 kg hammer mass*
- 1.5 cm head diameter

The aim of exciting the structure under investigation is to generate a certain force level over a specified frequency range. An impact input e.g., using a hammer generates relatively smoothly evolving force level up to a specific frequency. The hammer instrumented with a force transducer is as shown in the Fig 3.2.

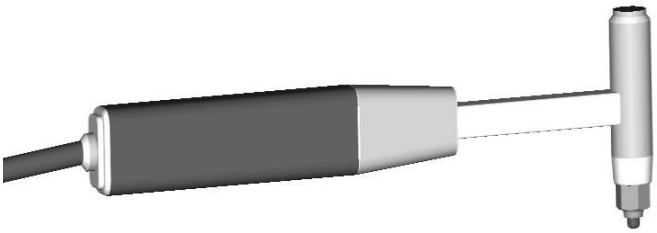

Figure 3.2: Impact hammer

Force and Motion Transducers

Once the structure is vibrating due to an induced force, from a fixed exciter or a hammer impact, input and output quantities to the mechanical system need to be measured. The systems input generally are the forces. Force transducers will measure these input forces. The system outputs generally are the displacements, velocity or accelerations at various locations of interest on the structure. Motion transducers will measure these outputs.

Force Transducers: Fig 3.3 shows the principle construction of a piezoelectric force transducer. The force acting on the transducer deforms the piezoelectric

crystal, thus generating a charge over the crystal. The main characteristics are the maximum force, minimum and maximum frequency (which depends on the load) and sensitivity. The force range is between 0.0005 and 250000 N. the mass is ranging from 8gms to 550gms.

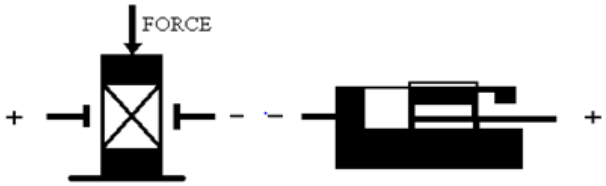

Figure 3.3: Piezo electric force transducer

Motion Transducer: In this experimental setup an ICP accelerometer is used, which is most often used in industries, mounted on the spindle. "ICP" is an acronym for internal integrated Circuit Pre-amplifier ICP accelerometer is a voltage mode sensor, which has built-in electronics. This is powered by constant current DC voltage source. Due to the low impedance voltage output the setup is less sensitive to the external influences than charge mode sensors. The Fig 3.4 shows the ICP accelerometer and specification of this accelerometer is given in the Table 3.1.

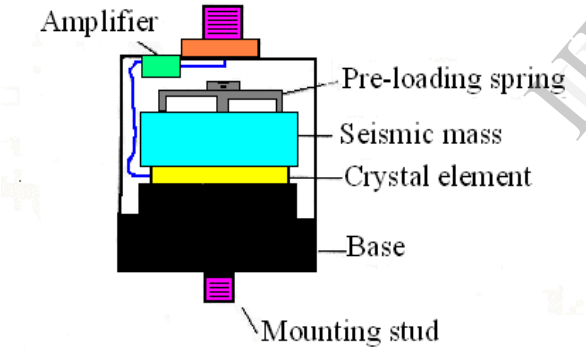

Figure 3.4: Accelerometer

Lower mass of accelerometer will have a much smaller adverse influence when attached to the structure and the results are more accurate. An additional factor that underlines the benefit of accelerometers is the factor that an acceleration signal can easily and validly be integrated electronically to obtain velocity and displacement. When the accelerometer is moved in the up and down direction, the force required to move the seismic mass is borne by the active element. According to Newton's second law, this force is proportional to the mass. The force on the crystal produces the signal, which is therefore proportional to the acceleration of the transducer.

Table 3.1: Specification of accelerometer

Measurement Range	± 490 m/s^2
Frequency Range	0.33 to 10000 Hz (± 3dB)
Temperature Range	-54° to + 121° C
Settling Time	<10 sec
Excitation voltage	18 to 28 VDC
Constant current excitation	2 to 20 mA
Size (Hex × Height)	22 mm × 109 mm
Weight (without cable)	94 gm.
Sensing element	Quartz
Housing material	Stainless steel
Sealing	Welded hermetic
Cable length	3.0 meters
Cable type	Polyurethane

3.2 Mounting Techniques

Mounting the accelerometer on the specimen is an important factor, which affects the operating range of accelerometer. The resonant frequency of an accelerometer is strongly dependent on its mounting technique. Fig 3.5 shows the assorted mounting configurations and their effects on high frequency. In this work the mounting base is made of aluminum. The underside of aluminum mounting base is machined to suit the curved surface of the spindle. It is fixed on the spindle with help of an adhesive. The accelerometer is stud-mounted to this aluminum base.

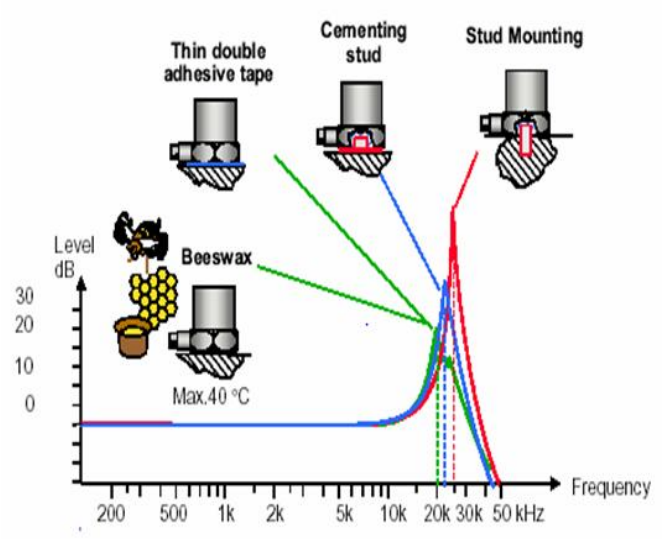

Figure 3.5: Assorted mounting configuration

4. Results and Discussion

4.1 Averaging in FFT Analyser

Time Response of Input

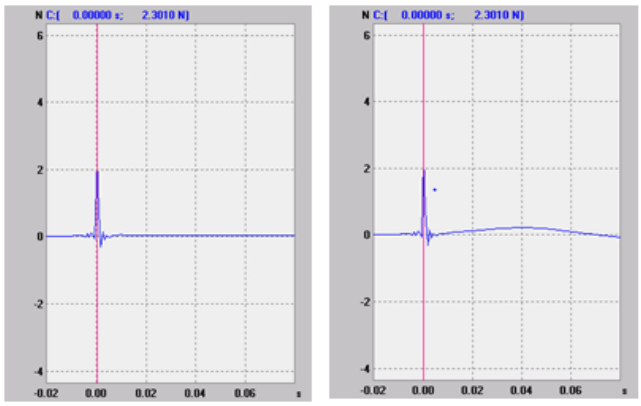

Figure 4.1: Trigger weighted CH-1 and Trigger CH-1

The impact input signal is transient deterministic signal consisting of a pulse lasting only a very small part of the sample period. Peak of the graph is the maximum amplitude of force applied. The bumps occurring after are due to the external disturbance like noise, air impact etc. These are avoided by considering only a part of time excluding the effect of bumps as shown in the trigger-weighted CH-1.

Time Response of Output

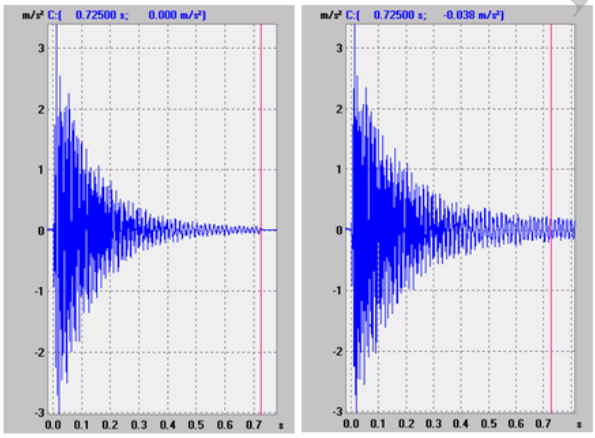

Figure 4.2: Trigger weighted CH-2 and Trigger CH-2

The response for the given input is as shown in the above graph. As it is evident from the graph the response is decreasing in its amplitude with increasing in time due to damping owing to the inter molecular friction of a material i.e. material damping. The interested length of time response is considered for analysis as shown in trigger-weighted CH-2.The logarithmic decrement can be calculated using the response for a known period. From the logarithmic decrement one can calculate the damping factor.

Spectrums

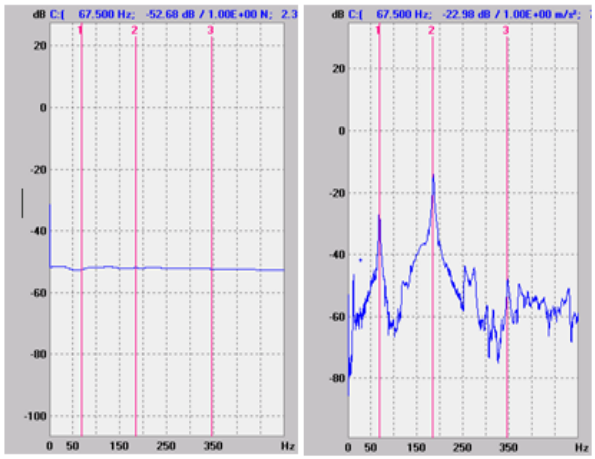

Figure 4.3: Spectrum of input force (Impact) and Spectrum of response (Acceleration)

The **Impact Force** spectrum will not show dips at the resonance of the structure. The shape width and amplitude of the pulse of force in the time wave form will determine the frequency content of the force spectrum. The shape and the amplitude mainly control the level of spectrum. The width controls the base band frequency span. The maximum frequency is inversely proportional to the width of the pulse.

The Acceleration **Spectrum** shows the peaks at the resonant frequencies of the structure. Near the frequencies the acceleration is very high that is almost linear. Other response points have acceleration well below the level of those points of resonance.

Frequency Response Function

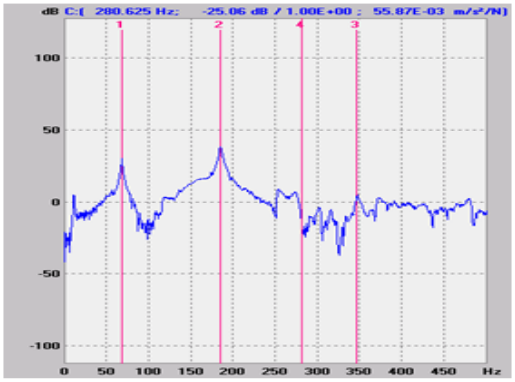

Figure 4.4: FRF CH- 2 / CH-1

The frequency response functions (FRFs) are functions of the characteristics of the system, and are independent of the input type. Assume linearity, time invariance absorbability and reciprocity when calculate FRFs. In this work measure FRFs between a reference transducer and response transducers. The FRFs contain amplitude and phase information. The operating condition has to be steady state since average the data to get FRFs. The FRF magnitudes have peaks at the system at the resonance and dips at the system anti resonance's.

Coherence

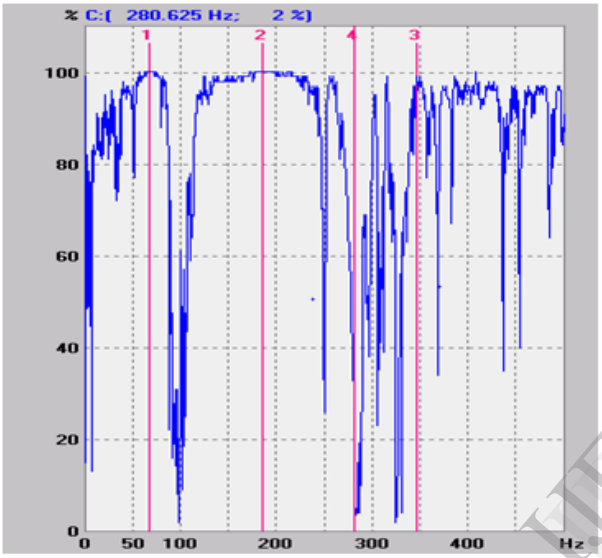

Figure 4.5: Coherence

Coherence is the extent up to, which the system is responding only to the input force and not to the any other force. At resonance, it is evident from the Fig 4.5 that, the coherence is almost 100 percent, but at anti resonance coherence is very low. This is because at resonance, the system operates with high response or amplitude. At anti resonance due to lower signal to noise ratio at these frequencies coherence is low. For better result the coherence must be good.

4.2 Estimation of Modal Parameters

Once the FRF's are estimated from the input and output data and updated, the next step would be calculation of modal parameters from the measured FRF's. There exist a number of modal analysis methods which, although different in their detail, all share the same basic assumption: namely, that in the vicinity of a resonance the total response is dominated by the contribution of the mode whose natural frequency is closest. The simplest method is one, which has been used for a long time and sometimes referred to as the '**peak-picking'** method or '**peak-amplitude**'. The method is applied as follows:

a) Natural Frequency

It is well known that each mode of vibration the system has specific natural frequency and damping factors. These natural frequencies can be obtained from FRF graphs. The peaks in the graphs represent the natural frequency provided the coherence at that peak should be very good; it is expected to be above 95%. Sharpness of the peak implies low damping.

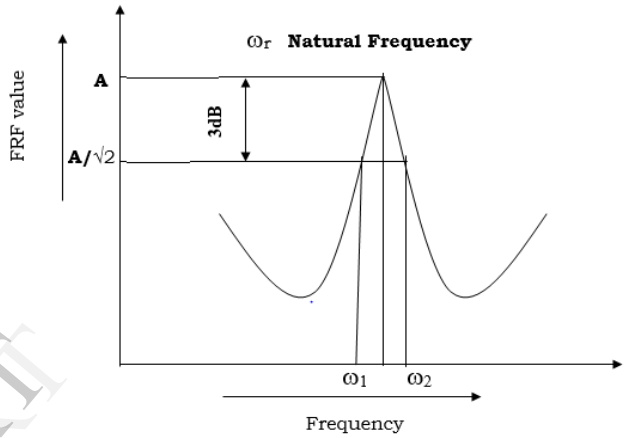

Figure 4.6: Natural frequency

b) Damping Factor

As it is known, for each mode of vibration there is a specific damping factor. Modal damping factor can be calculated from the FRF graph (Fig 4.6) and the structural damping from the time response shown in the Fig 4.7. In time response first calculate the logarithmic decrement and then using the known relation (Eq. 4.2) calculate damping factor. The maximum value of the FRF is noted, as A and the frequency bandwidth of the function for a response level of A/√2 is determined. The two thus identified as ω_2 and ω_1, are the "half power points" as shown in the Fig 4.6. Using FRF graphs modal damping can be calculated using Eq. 4.1.

$$Damping\ Factor = \xi = \frac{W_2 - W_1}{2 \times W_r} \qquad Eq.4.1$$

Structural damping can be calculated using equation 4.2

$$Logarithmic\ Decrement\ (\delta) = \delta = \frac{1}{n} ln \left(\frac{X_n}{X_{n+1}}\right) = \frac{2 \times \pi \times \xi}{\sqrt{1 - \xi^2}} \qquad Eq.4.2$$

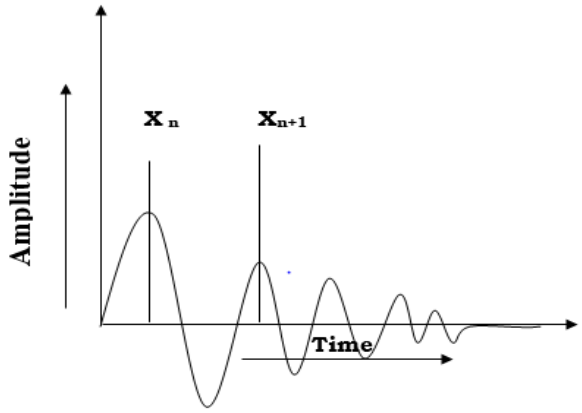

Figure 4.7: Decaying Time Response

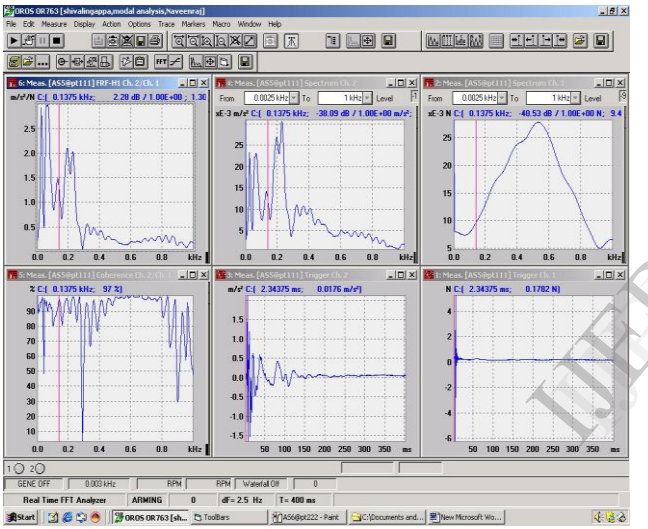

Figure 4.8: Al-SI5 at point 1

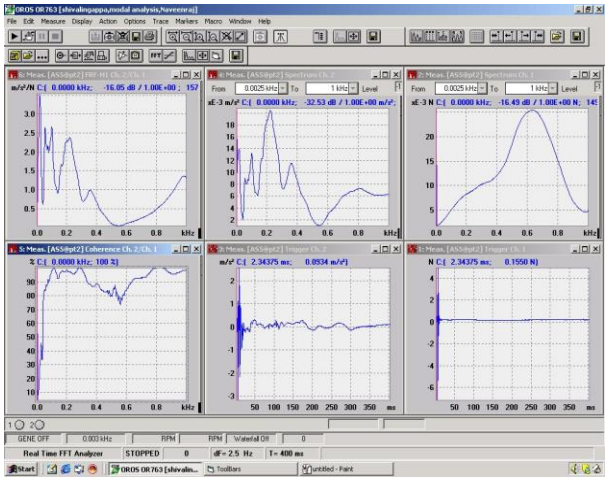

Figure 4.9: Al-Si5 at point 2

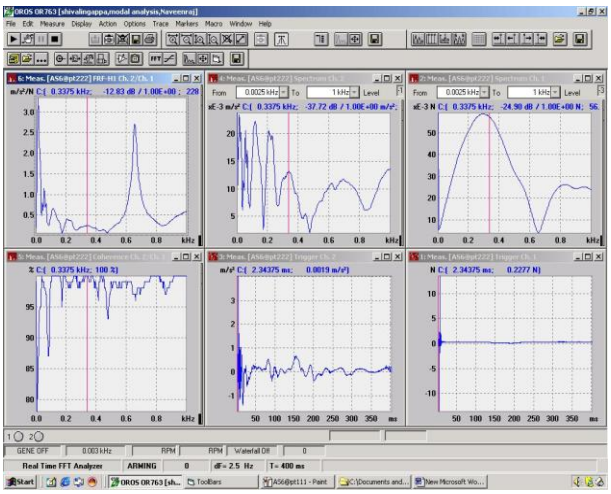

Figure 4.10: Al-Si6 at point 1

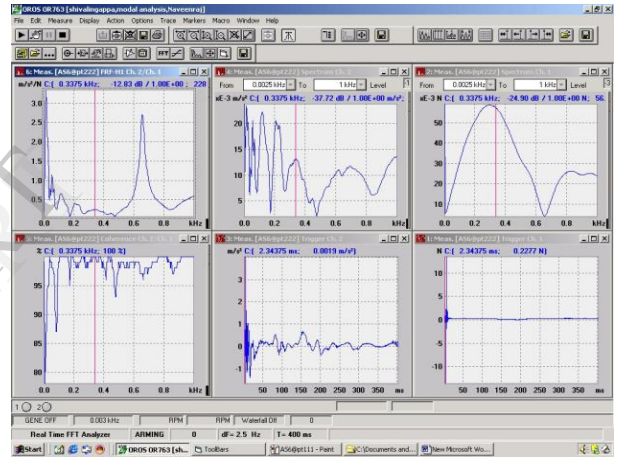

Figure 4.11: Al-Si6 at point 2

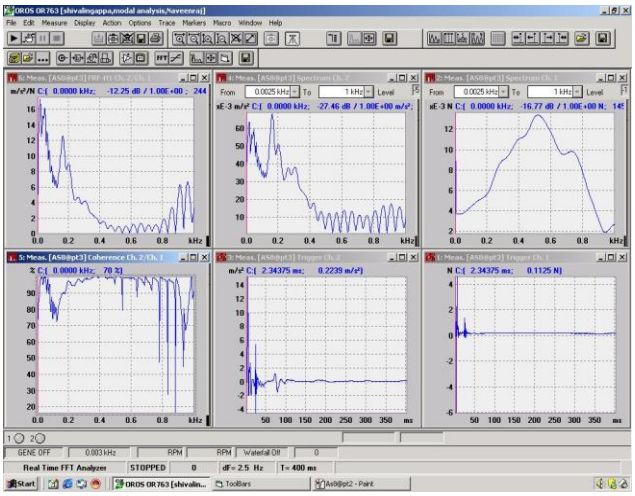

Figure 4.12: Al-Si8 at point 1

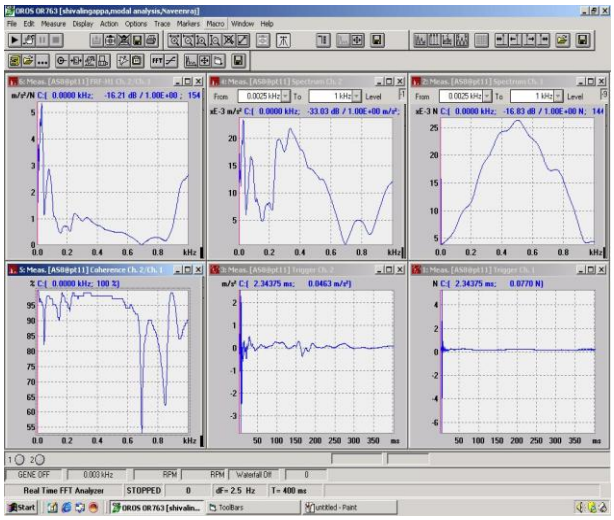

Figure 4.13: Al-Si8 at point 2

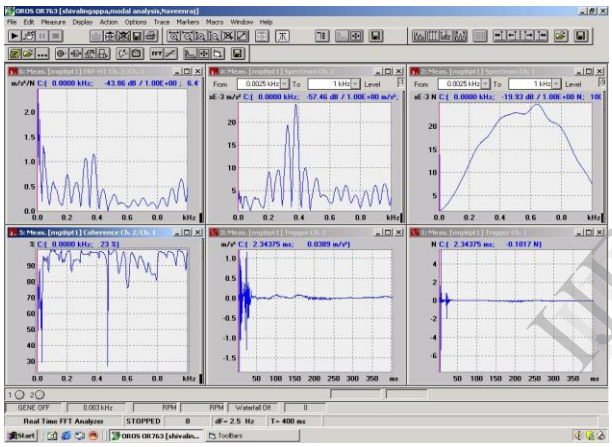

Figure 4.14: Mg at point 1

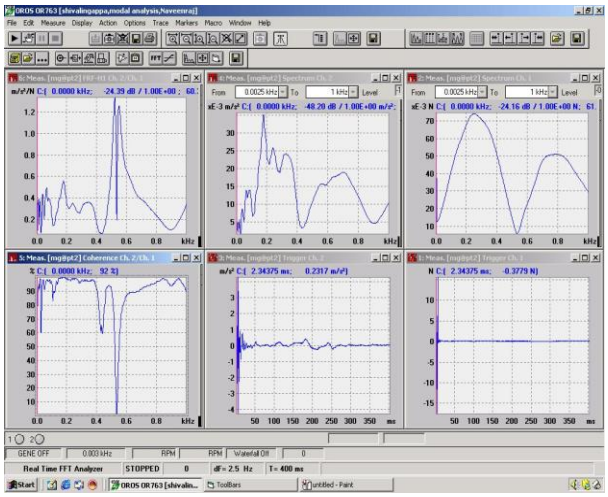

Figure 4.15: Mg at point 2

4.3 Analytical Modal Analysis

The study of the dynamic characteristics such as mode shapes and natural frequencies are alloys. Solid model was created in ANSYS using solid 186 element and link 1 elements were introduced at the suspension points on the material as shown in Table 4.1.

Table 4.1: Material Properties

	Young's modulus $N/(mm)^2$	Density m/sec^2	Poisson's ratio
Magnesium(pure)	41000	1.74e-6	0.35
Al –Si5	80000	2.66e-6	0.30
Al-Si6	85000	2.67e-6	0.25
Al-Si	90000	2.63e-6	0.25

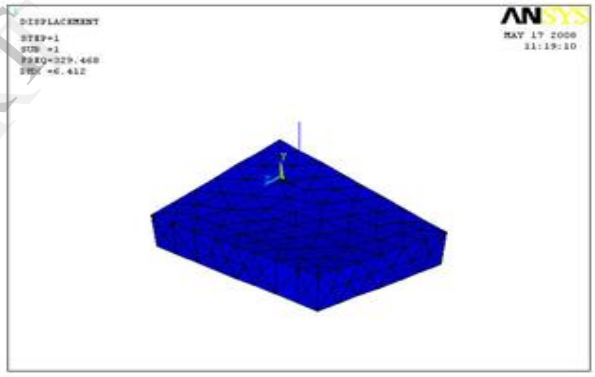

Figure 4.16: Mode shape at natural frequency 329.468 Hz

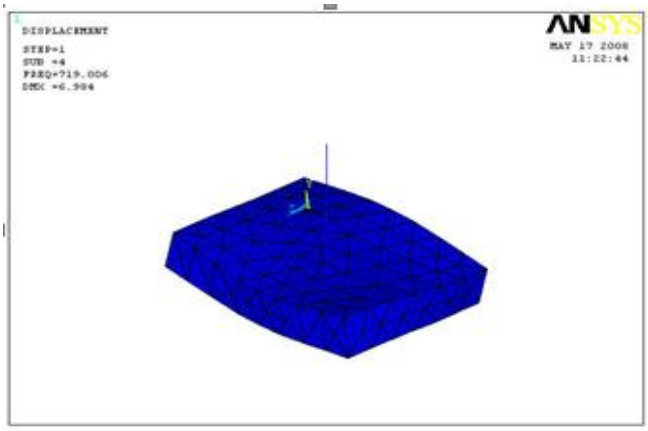

Figure 4.17: Mode shape at natural frequency 719.006 Hz

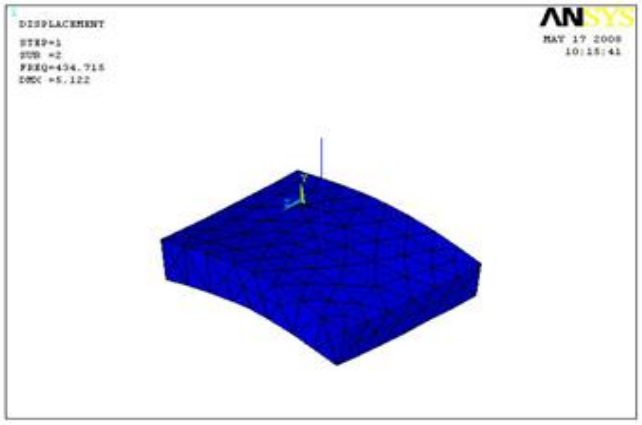

Figure 4.18: Mode shape at natural frequency 434.715 Hz

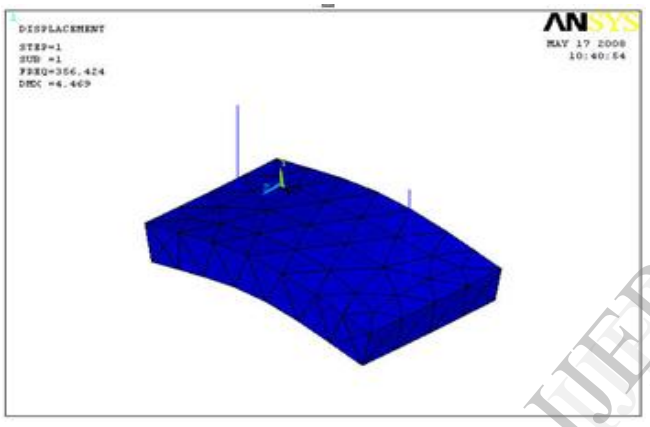

Figure 4.19: Mode shape at natural frequency 705.50Hz

5. Validation

Damping factor at various Modal frequencies and composition are shown in the Fig 5.1 and 5.2.

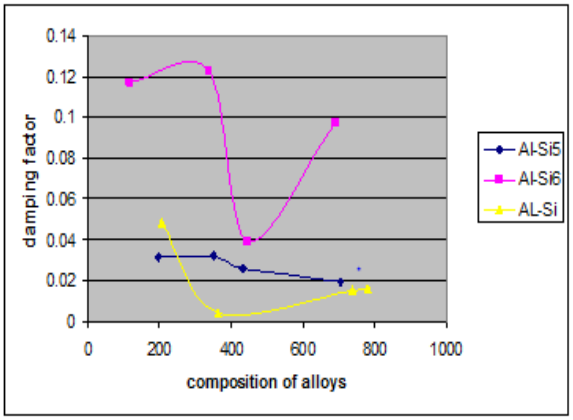

Figure 5.1: Variation of damping factor for various composition of Al-Si

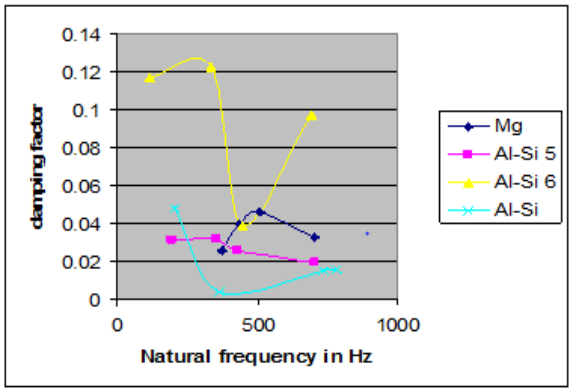

Figure 5.2: Variation of damping factor for different modes of vibration

5.1 Comparison of Natural Frequencies

The most obvious comparison to make is of the measured against the predicted natural frequencies. This is often done by a simple tabulation of the set of results but more usual format is by plotting the experimental values against the predicted one for each of the modes included in the comparison as shown in the figure and table. In this way it is possible to see not only the degree of co-relation between the two sets of results, but also the natural and possible cause of any discrepancies that do exist. The points plotted should lie on or close to straight line of slope. If they lie close to line of different slope then almost certainly the cause of discrepancies is the erroneous material properties used in the prediction. If the points lie scattered widely about straight line than there is a serious failure of model to represent is the test structure and a fundamental re-evaluation is called for. If the scattered is small and randomly distributed than this may be expected from a normal modelling and measurement process.

Comparison of Modal Frequencies of Commercial Magnesium

Mode No.	Experimental Frequencies Hz	Analytical Frequencies Hz
1	356.42	340.00
2	412.50	414.68
3	562.50	562.29
4	832.27	832.50

Comparison of Modal Frequencies of Al-9 wt % Si

Mode No.	Experimental Frequencies Hz	Analytical Frequencies Hz
1	320.00	329.47
2	425.00	421.24
3	687.50	692.64
4	720.00	719.01

Comparison of Modal Frequencies of Al-6 wt % Si

Mode No.	Experimental Frequencies Hz	Analytical Frequencies Hz
1	342.50	345.40
2	440.00	434.71
3	692.50	705.50
4	750.00	749.32

Comparison of Modal Frequencies of Al-15 wt % Si

Mode No.	Experimental Frequencies Hz	Analytical Frequencies Hz
1	357.50	358.10
2	467.50	450.75
3	737.50	731.45
4	780.00	776.88

6. Conclusion and Remedies

Data obtained with experimental technique and data from the finite element model are often not compatible mainly for the following reasons:

i. Measured degrees of freedom do not coincide with the degree of freedom in the finite element model: The matching step in the updating procedure provides an approximate, solution for this problem.

ii. The set of experimental modal data is incomplete: Not only the number of experimental degree of freedom is limited, but also the set of modal data is limited. The measurement of frequency response functions is performed but in a limited bandwidth. Hence the set of identified modal data is incomplete.

iii. Noise contaminates measurement:

Relative errors of 3% on resonance frequencies, relative errors of 10% on the components of mode shapes and relative errors of 30% on modal masses and stiffness are considered to be acceptable. It is obvious that the use of erroneous experimental data gives misleading indication in the correlation and the error localization step and the causes the correction step to converge to inaccurate and meaningless values. Most often the experimental modal masses and stiffness are not used in the updating procedure.

iv. Damping cannot be included accurately in the finite element model: Damping information is inherently present in the experimental data but often neglected in the finite element model. As a consequence, an undamped finite element model is updated by means of experimental data of a damped structure. It is obvious that this discrepancy can cause errors in the updating process. Mode normalization techniques are an approximate way to avoid the difficulty.

References

[1] M.A. De Buergo., C.Vazquez-Calvo, R Fort,(2011) The measurement of surface roughness to determine the suita bility.Geophysical Research Abst.; 13: 6443-6444.

[2] M.J. Caton ,J.W. Jones ,H. Mayer ,S. Stanzl ,J.E.(2003) Allison Demonstration of a

endurance limit in 319 aluminum, J. Chem. Mater. Sci.; 34:33- 40.

[3] N.B. Nadu . T.V.Bi . (2007) Effect surface roughness on the hydro dynamic lubrication of one dimensional. Poro.;15:278-286.

[4] Menezes P.L., K., K.S.V., (2008). Surface texture and thus roughness parameters influence coefficient of friction under lubricated conditions. Wear .33, 181–190.

[5] K.J. Kubiak, T.G. Mathia, S. Fouvry,(2010). Interface roughness effect on friction map under fretting contact Conditions'. J. Tribology Internet Vol. 43, p. 1500-1507

[6] Kadirgama K., Noor M., Raman M.M., (2009). Surface Roughness Prediction Model 6061-T6. J. Scientific Research. 25, 250-256.

[7] Takata R ., (2006.) Effects of small-scale texturing on ring liner friction Victor, Sacramento CA, USA.

[8] W. Wieleba .(2002) The statistical correlation of the coefficient of friction and wear rate of PTFE composites. J. Wear; 252:719–729.

[9] H J M. C., (2000) Chapter 10 of 'Cast and ought Aluminum Bronzes Properties, Processes and Structure 'Resistance to Wear of Aluminum Bronzes CD Publication Pub 1266,

[10] Gary Vosler(2006). Coefficient of static friction (slide angle) of packaging and packaging materials (including shipping sack papers, corrugated and solid fiberboard) (inclined plane method) T 815: 50308.03.

[11] K. V. Arun and K.V. Swetha .,(2011). Influence of Material Condition on the Dry Wear Behavior of Spring Steels Journal of Minerals &Materials Characterization & Engineering,10:323-337.

[12] H. Czichos, K.-H. Habit,(2003).Tribological-Handbook (Tribological handbook)Viewer Velar, Wiesbaden n,2nd edition, I SBN.3-528-16354-2,

[13] P.L. Menezes ,K.S.V. K (2008)Surface texture roughness param. influence coef.,; 33: 181 – 190.

[14] K.J. Ku , T.G. Math. (2010) Interface roughness effect friction map under fretting Contact Condi. Tribogy In ternational ;43:1500 -1507

[15] K. Kadirgama M. Noor M.M. Raman . (2009)Surface Roughness Prediction Model 6061- T6. J. Scientific Research,; 25:250-256.

[16] Y.A. Karpenko , A, Akay . (2001)Mechanical Enginee ing, A numerical model of friction between rough surfaces. Tribology International; 34: 531–545.

[17] P. Xing . B. Gao .Y. Zhuang .K. Liu .G. Tu.(2010) On the medication of hypereutectic Al - Si alloys using Er,Acta Metall .Sin.(Engl.Lett.) 23:327- 333.

[18] M.Gupta .S. Ling . (1999) Microstructure and mechanical proper ties of hyp/hypereutectic Al–Si alloys synthesized us ing a near- net shape forming technique, J. Alloys; 287:284–294

[19] Paulus S.,Jyrki H., Jukka R., and Jouko Y.,(2006) Monitoring Tablet Surface Roughness During the Film Coat ing Process., J.AAPS PharmSciTech; 7 (2) Article 31.

[20] Mitjan K., Said J., (2003) Influence of roughness on wear transition in glass-infiltrated alumina , Wear 255 669–676

[21] K.J. Kubiak , T.W. Liski., T.G. Mathia(2011) ., Surface morphology in engineering applications: Influence of roughness on sliding and wear in dry fretting J. Tribology International l, 44 p.1427-1432,